ACS NANO
Cite This: ACS Nano XXXX, XXX, XXX–XXX
www.acsnano.org

ARTICLE

Triboelectric-Nanogenerator-Based Soft Energy-Harvesting Skin Enabled by Toughly Bonded Elastomer/Hydrogel Hybrids

Ting Liu,[†,‡] Mengmeng Liu,[†,‡] Su Dou,[§] Jiangman Sun,[†,‡] Zifeng Cong,[†,‡] Chunyan Jiang,[†,‡] Chunhua Du,[†,‡] Xiong Pu,*[,†,‡] Weiguo Hu,*[,†,‡] and Zhong Lin Wang*[,†,‡,∥]

[†]CAS Center for Excellence in Nanoscience, Beijing Institute of Nanoenergy and Nanosystems, Chinese Academy of Sciences, Beijing 100083, China

[‡]School of Nannoscience and Technology, University of Chinese Academy of Sciences, Beijing 100049, China

[§]University of Science and Technology Beijing, Beijing 100083, China

[∥]School of Materials Science and Engineering, Georgia Institute of Technology, Atlanta, Georgia 30332-0245, United States

Supporting Information

ABSTRACT: **A major challenge accompanying the booming next-generation soft electronics is providing correspondingly soft and sustainable power sources for driving such devices. Here, we report stretchable triboelectric nanogenerators (TENG) with dual working modes based on the soft hydrogel−elastomer hybrid as energy skins for harvesting biomechanical energies. The tough interfacial bonding between the hydrophilic hydrogel and hydrophobic elastomer, achieved by the interface modification, ensures the stable mechanical and electrical performances of the TENGs. Furthermore, the dehydration of this toughly bonded hydrogel-elastomer hybrid is significantly inhibited (the average dehydration decreases by over 73%). With PDMS as the electrification layer and hydrogel as the electrode, a stretchable, transparent (90% transmittance), and ultrathin (380 μm) single-electrode TENG was fabricated to conformally attach on human skin and deform as the body moves. The two-electrode mode TENG is capable of harvesting energy from arbitrary human motions (press, stretch, bend, and twist) to drive the self-powered electronics. This work provides a feasible technology to design soft power sources, which could potentially solve the energy issues of soft electronics.**

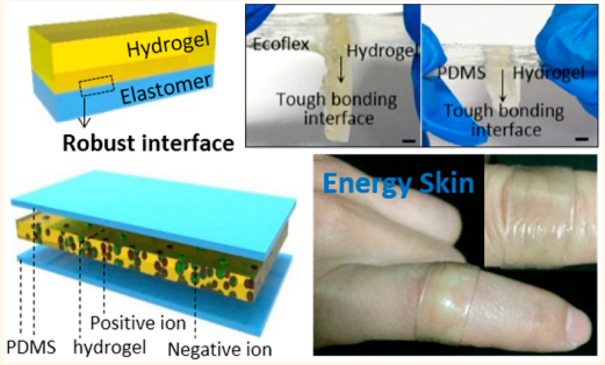

KEYWORDS: *triboelectric nanogenerator, soft electronics, hydrogel, energy harvesting skin, tough bonding*

Next-generation electronics will be soft, deformable, and biocompatible, enabling appealing applications that are hardly achieved by today's hard and brittle electronics. State-of-art examples range from electronic skins for smart sensing and healthcare,[1−4] soft robotics,[5] flexible/stretchable optoelectronic devices,[6−8] and smart textiles,[9,10] to soft biomedical devices.[11,12] Their deformable and biocompatible characteristics allow their intimate integration with the human body, providing great potential in wearable and biomedical applications.[13−15] Nevertheless, an accompanying big challenge is providing correspondingly stretchable and sustainable power sources for such devices, especially soft/stretchable energy-harvesting devices that can convert environmental energies into electricity.[16]

Recently, triboelectric nanogenerators (TENGs) have been developed as highly efficient and sustainable power sources by transforming ambient mechanical energy into electrical output.[17−24] Considerable attempts have been made to develop flexible TENGs to harvest various forms of mechanical energies, especially the energies of human motions.[25−27] In particular, stretchable and transparent TENGs are highly demanded since wearable TENGs are frequently required to deform accordingly with human motions without deterioration of device performance,[28] and transparency helps potential application in the visual transmission of information.[29−31] Typically, thin dielectric polymer films and conductive films (metal, graphene, indium tin oxide, *etc.*) are applied as the triboelectrification layers and electrodes, respectively. Several studies have also demonstrated stretchable TENGs by using

Received: January 5, 2018
Accepted: March 1, 2018
Published: March 1, 2018

DOI: 10.1021/acsnano.8b00108
ACS Nano XXXX, XXX, XXX–XXX

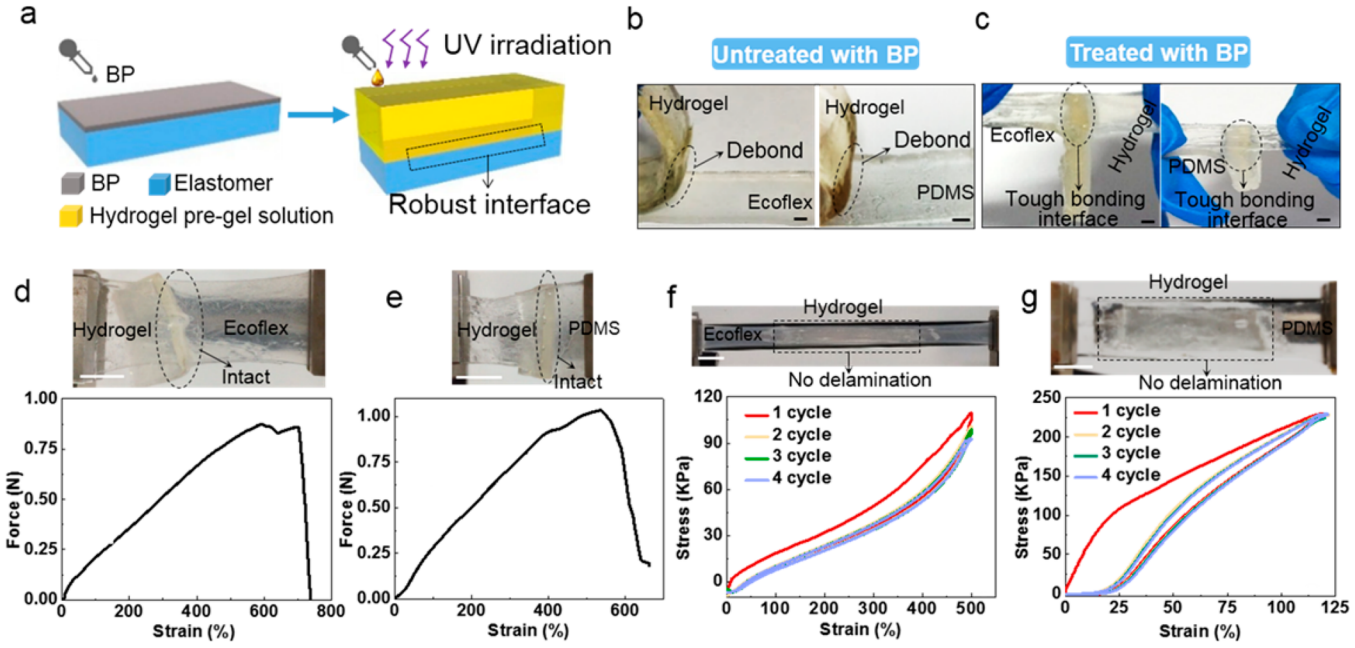

Figure 1. Fabrication of toughly bonded elastomer/hydrogel hybrids. (a) Schematics of a practical fabrication approach for robust hydrogel-elastomer hybrid. Photographs showing (b) the easily debonded elastomer/hydrogel interfaces without BP treatment and (c) tough bonding interfaces after BP treatment. Photographs and stress−strain curves of tensile tests of the (d) hydrogel−Ecoflex and (e) hydrogel−PDMS hybrid. Photographs and stress−strain curves of cyclic tensile tests of the (f) hydrogel−Ecoflex and (g) hydrogel−PDMS hybrid. Scale bars are 1 cm.

rubbery elastomers as the electrification layer.[32,33] Percolated conductive networks,[34] liquid phase conductors,[35] or woven entangled metal yarns[36] have been employed as the stretchable electrodes. Our last work achieved ultrahigh stretchability (ultimate uniaxial strain of 1160%) for skin-like TENG based on stacked hybrids of elastomers and ionic hydrogels.[37] Furthermore, this material combination ensures the biocompatibility, environmental friendliness, and low cost as well,[38,39] making the resulting TENGs highly suitable as power sources for electronics related to smart skins, soft robotics, or wearable/biomedical applications. However, the weak adhesion between the conductive hydrogel and electrification elastomer in the TENG greatly reduces its mechanical reliability. The hydrophilic hydrogel and the generally hydrophobic elastomers naturally form a weakly bonded interface, which is still a fatal drawback to the TENG-based energy harvesting skins.[37]

Here, we report stretchable TENGs with dual working modes based on the soft hydrogel-elastomer hybrid as the energy skin for biomechanical energy harvesting. The robust bonding between the hydrogel and elastomer, achieved by the interface modification with benzophenone (BP) upon ultraviolet (UV) irradiation, was confirmed by the debonding tensile test and cyclic tensile loading test. Contrary to the uncoated hydrogel, the average dehydration rate of the hydrogel−elastomer hybrid can decrease by 73.2%−78.6% in an environment of an average relative humidity (RH) of ∼26% at 30 °C, enabling its potential application in harsh environments. With polydimethylsiloxane Sylgard 184 (PDMS) as the electrification layer and polyacrylamide−sodium alginate (PAAm−alginate) hydrogel as the electrode, a stretchable, transparent (90% transmittance) and ultrathin (380 μm) single-electrode TENG was fabricated to conformally attach on human skin for harvesting human motion energies. The two-electrode contact-separation mode TENG is also developed to drive the self-powered electronics with energies converted from arbitrary human motions (press, stretch, bend, and twist). This work provides a feasible technology to design soft power sources, which could potentially solve the energy issues of the next-generation soft electronics.

RESULTS AND DISCUSSION

The interfacial bonding strength between the PAAm-alginate hydrogel and the elastomer films is naturally weak, because the hydrogel is hydrophilic and elastomers are typically hydrophobic. One of the effective approaches to improve such a problem is modifying polymers' surfaces through BP.[40−42] The process begins with treating elastomer by BP in ethanol solution, and then adding hydrogel presolution to the elastomer followed by UV irradiation (Figure 1a). When excited by UV irradiation, the photochemically produced triplet state of BP can abstract hydrogen atoms from superficial elastomer polymers and then generate methyl radicals.[40,41] Thus, the radical can act as an initiator for polymerization of the hydrogel polymer onto the reactive sites on the elastomer surface, leaving benzopinacol as a final reaction product (Supporting Information Figure S1).[43] As a result, the robust bonding interface forms due to the covalently cross-linking hydrogel polymers on elastomer surfaces. As confirmed by the optical images in Figure 1b, the hydrogel can be easily detached from elastomers (both Ecoflex and PDMS); while elastomer−hydrogel hybrid with the BP interface treatment can hardly be debonded by hand (Figure 1c).

To quantitatively demonstrate the robust toughness between the hydrogel and the elastomer, multiple kinds of tensile tests were carried out. As shown in Figure 1d, one end of a hydrogel film (4 cm × 1.8 cm × 1 mm) was bonded on an Ecoflex film (4 cm × 1.8 cm × 1 mm) with the interface treatment, and the free ends of the two films were fixed on the two holders of a tensile tester, respectively. When the tensile stress reaches the

DOI: 10.1021/acsnano.8b00108
ACS Nano XXXX, XXX, XXX−XXX

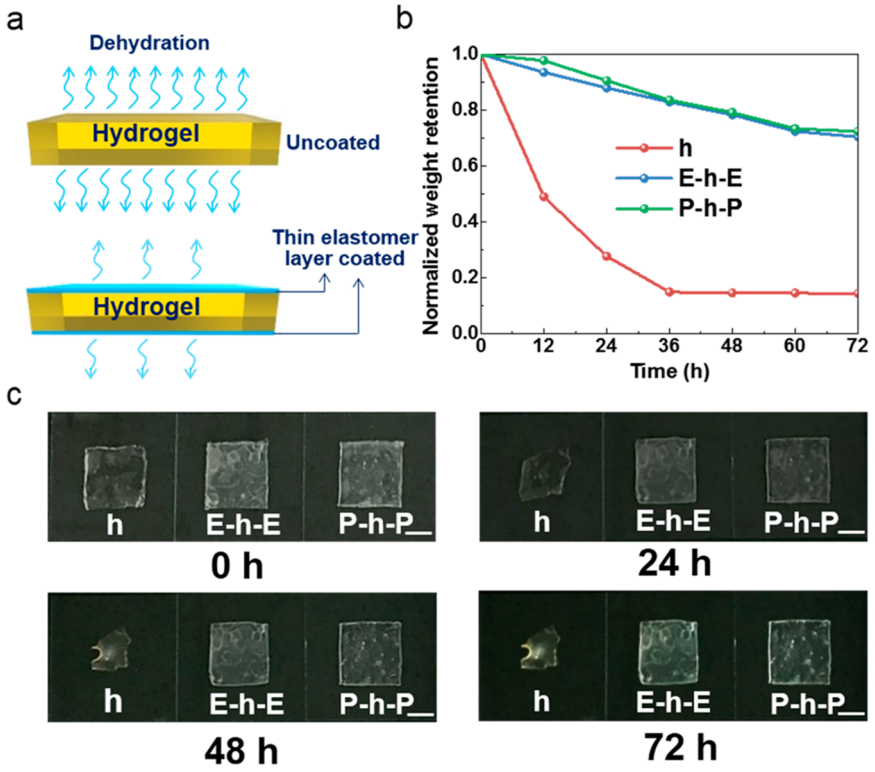

Figure 2. Antidehydration performances of toughly bonded hydrogel/elastomer hybrids. (a) Schematic diagram of the antidehydration of stacked elastomer/hydrogel. (b) Normalized weight retention of the uncoated hydrogel, Ecoflex–hydrogel–Ecoflex (E-h-E), and PDMS–hydrogel–PDMS (P-h-P) kept at a dry environment with a RH of 26% at 30 °C. (c) Optical images of the hydrogel–elastomer hybrids and bare hydrogel during the dehydration experiments. Scale bars are 1 cm.

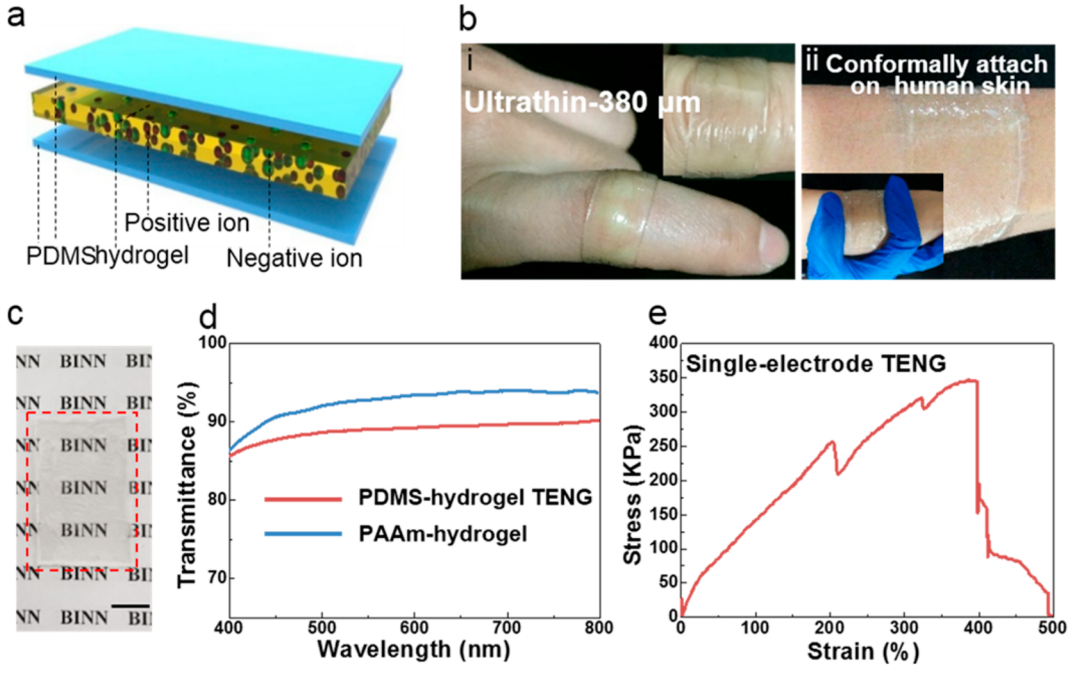

Figure 3. Fabrication of single-electrode stretchable and transparent TENG. (a) Scheme of the single-electrode TENG with sandwich structure. (b) Optical images of an ultrathin energy skin conformally attached on (i) a bended finger and (ii) an arm. (c) Optical image of the highly transparent single-electrode TENG. (d) Transmittance of the single-electrode TENG in the visible range. (e) Uniaxial tensile test of the hydrogel-PDMS single-electrode TENG. Scale bar is 1 cm.

limit load (strain up to 740% at 0.88 N, strain velocity is 70 mm/min), the free hydrogel film fractures but the bonding interface of the hybrid still remains intact. Similarly, the PDMS-hydrogel interface bonding is also intact even after the fracture of the free hydrogel film (Figure 1e). In addition, the robustness of hydrogel-elastomer hybrids can also be validated

DOI: 10.1021/acsnano.8b00108
ACS Nano XXXX, XXX, XXX–XXX

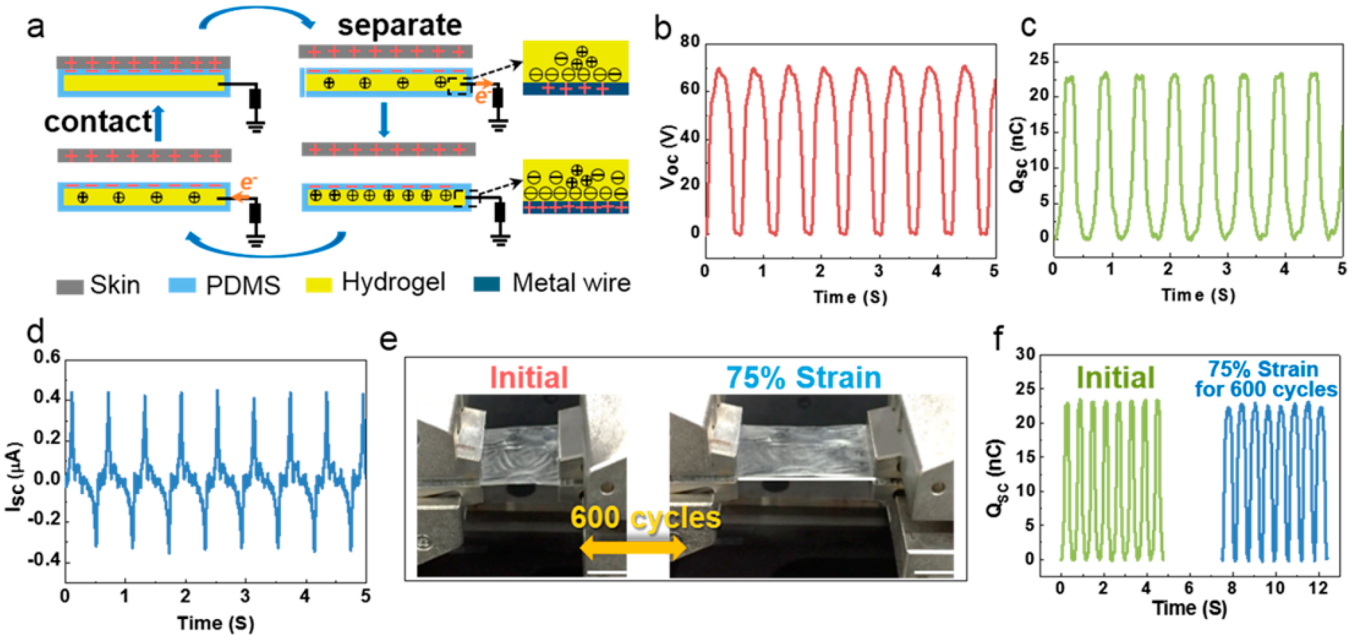

Figure 4. Electricity generation of the single-electrode soft TENG. (a) Scheme of the working mechanism of the single-electrode PDMS-hydrogel TENG. (b) V_{OC}, (c) Q_{SC}, and (d) I_{SC} of a hydrogel–PDMS single-electrode TENG. (e) Optical images of the TENG at the initial state and 75% strain state. (f) Comparison of the output Q_{SC} of the TENG before and after being 75% strain for 600 cycles. Scale bars are 1 cm.

in other modes of deformation. An Ecoflex sheet (3 cm × 1.5 cm × 2 mm), with a hydrogel film (2 cm × 1 cm × 1 mm) coated at the central deforming area, still shows stable cyclic mechanical tensile performances with tensile strain up to 500% (Figure 1f). No delamination of the hydrogel film is observed throughout the course of the cyclic tensile test (the optical image in Figure 1f). Besides, the hydrogel–Ecoflex laminate fractures at an ultimate tensile strain of 792%, but the cross-section interface remains intact without observable damage (Figure S2a). Similar results of the hydrogel–PDMS hybrid are presented in Figure 1g and Figure S2b.

With rapid developments of hydrogel-based electronics, the dehydration of hydrogels becomes a critical issue in this field since the ionic conductivity and mechanical elasticity of the hydrogel will decrease along with time.[44] We carried out dehydration tests for the uncoated hydrogel, sandwiched Ecoflex–hydrogel–Ecoflex (E-h-E) hybrid and PDMS–hydrogel–PDMS (P-h-P) hybrid with the same dimensions (2.3 cm × 2.3 cm × 1.25 mm) under the constant ambient conditions (30 °C and 26% relative humidity (RH)) for 72 h. The schematic structure diagrams of these three samples are shown in Figure 2a. As shown in Figure 2b, the weight of uncoated hydrogel decreases rapidly in the first ~20 h, and maintains only 14.5% of its initial weight after 72 h, suggesting the depletion of the water content. The average dehydration rate reaches 11.2 mg/h. In contrast, the weight retention ratio of the E-h-E hybrid is finally 70.5%, corresponding to an average dehydration rate of 3.0 mg/h. The P-h-P hybrid retains 72.4% of its initial weight with an average dehydration rate of 2.4 mg/h. As compared with that of the bare hydrogel, the average dehydration rate has been reduced by 73.2% and 78.6% due to the coating of Ecoflex and PDMS, respectively. From the optical images (Figure 2c), it is clear that the size of the uncoated hydrogel has shrunken significantly and it even become curled, whereas, the appearance of the two hybrids has not changed evidently during the test. Thus, it is reasonable to believe that this excellent antidehydration performance ensures the proper function of the hydrogel–elastomer-based TENG in harsh environments.

The stretchable single-electrode TENG has a three-layer structure that the conductive hydrogel electrode is sandwiched by two PDMS thin films. Detailed fabrication methods are described in the Methods section. As shown in Figure 3a, the presence of high concentrations of positive and negative ions contributes to the high ionic conductivity (1.25×10^{-5} S/cm) of the hydrogel based on the electrochemical impedance spectroscopy (EIS) measurement (Figure S3a). Although the resistance of the electrode increases with the elongation strain (Figure S3b), this increase is acceptable and will have little negative impact on the TENG's performance, because the inherent impedance of TENG is much larger and at the scale of MΩ.[45] The highly transparent device (Figure 3c) has an ultrathin film structure with a thickness of only 380 μm, enabling it to be attached conformally onto a bended finger and wrinkled skin (Figure 3b). A 1 mm-thick hydrogel film achieves an average transmittance of 94% in the visible range from 400 to 800 nm. The single-electrode TENG shows an average transmittance of 90%, much higher than those of previously reported transparent TENG using graphene or indium tin oxide (ITO) (Figure 3d).[46−48] Uniaxial tensile tests are performed to evaluate the mechanical properties of the TENGs (Figure 3e). The single-electrode TENG starts to rupture at a stress of 344 kPa and the tensile strain of 397% (strain rate 70 mm/min).

Figure 4a schematically illustrates the working mechanism of the single-electrode TENG. Tribo-electrification together with the electrostatic induction effect contributes to the energy generation of the TENG.[23,49−51] According to the triboelectric series, PDMS and human skin can be considered as triboelectrically negative and positive materials, respectively, due to their different electronegativity.[52] Initially, the human skin keeps in contact with the PDMS layer, charges transfer from the human skin to the PDMS, making the PDMS layer

DOI: 10.1021/acsnano.8b00108
ACS Nano XXXX, XXX, XXX−XXX

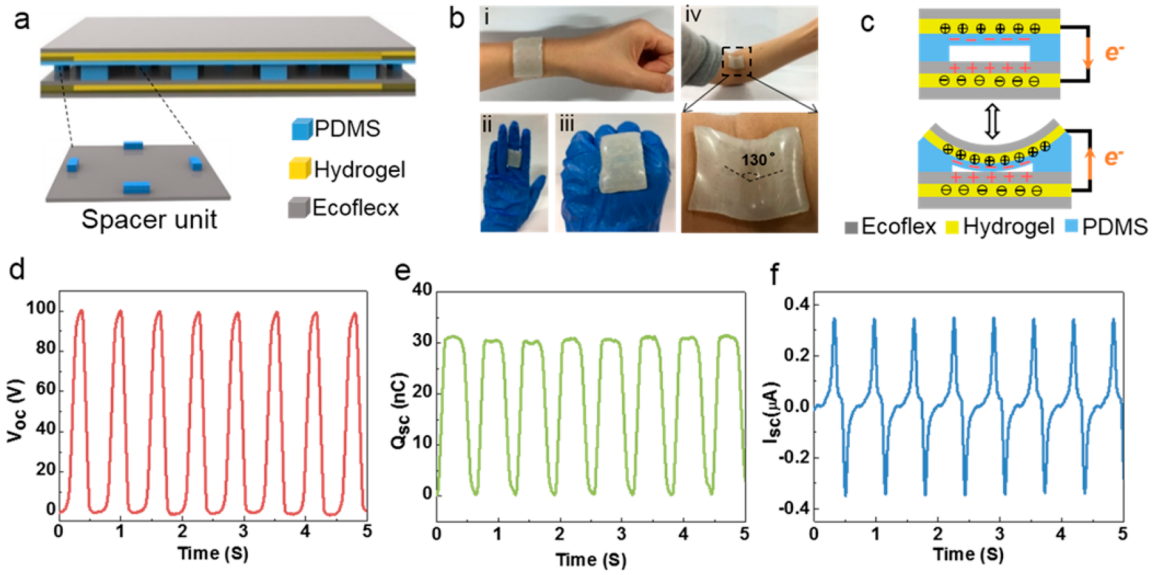

Figure 5. Fabrication and output characteristics of the two-electrode soft TENG. (a) Schematic diagrams of the two-electrode TENG with the PDMS spacers. (b) Photographs showing the shape-adaptive TENG conformly attached to various curvy surfaces of the human body. (c) Schematics of the working mechanism of the contact−separation TENG. (d) V_{OC}, (e) Q_{SC}, and (f) I_{SC} of the contact−separation TENG.

negatively charged, and the human skin positively charged.[32] When the skin is moved away from the PDMS, an electrical potential difference is built between the two separated oppositely charged surfaces.[53] The unscreened negative charges on the PDMS surface causes the accumulation of positive ions at the upper PDMS/hydrogel interface and negative ions at the bottom PDMS/hydrogel interface.[54] Then a transient charge flows from the Cu connecting wire to the ground, generating a current pulse. An electrostatic equilibrium is achieved when the human skin and the PDMS layer reach the maximum separation distance. As the skin moves back again, the process is reversed and a charge flow along the opposite direction occurs.[55,56] Thus, the continual contact−separation motion described above produces an alternative current. When the moving dielectric film remains in contact with the elastomer, both open-circuit voltage (V_{oc}) and short-circuit charge quantity (Q_{sc}) are 0. When the dielectric film is moving far away from the elastomer, V_{oc} and Q_{sc} can be derived as[57−59]

$$V_{oc} = -\sigma A/2C_o \quad (1)$$

$$Q_{sc} = -\sigma A/2 \quad (2)$$

where σ is the density of electrostatic charges generated at the surface of the elastomer film, C_o is the capacitance of the TENG, and A is the contacting area between the dielectric film and the elastomer film.

The energy-harvesting performance of the single-electrode TENG was evaluated by applying a cycling contact−separation motion. The frequency (1.5 Hz) and speed (0.2 m/s) of the compression cycle and the pressure (~100 kPa) between the two contacting films are controlled to be stable by a stepping motor for all following tests. The single-electrode TENG generated the approximate V_{oc} of 70 V (Figure 4b), Q_{sc} of 23.4 nC (Figure 4c), and I_{sc} of 0.46 μA (Figure 4d). To investigate the actual output power of the soft TENG, we obtained load matching curves by using an external load resistor varying from 100 Ω to 1000 MΩ. As the resistance increases, the current density amplitude decreases while the output power density of the device reaches the peak value of 135 mW/m^2 at the optimum load resistance of 800 MΩ (Figure S4a). Besides, the single-electrode TENG with ionic hydrogel as the electrode shows no mechanical fatigue or degradation in electrical output under a 75% strain for 600 cycles (Figure 4e,f). In addition, the stability of the single-electrode TENG was also characterized by the long-term motion cycles as shown in Figure S4b. It is clearly seen that the output voltage of the TENG does not exhibit obvious change after ~5000 cycles (for 60 min) of repeated contact−separation motion. The excellent mechanical stability satisfies the needs of reliability for a practical nanogenerator.[46]

A two-electrode soft TENG working at contact−separation mode has also been developed for the application where the grounding is inconvenient. The structure of the contact−separation mode TENG is schematically depicted in Figure 5a. Two PAAm−alginate hydrogel films both sealed inside two elastomer layers are employed as the top and bottom electrodes. The middle Ecoflex and PDMS films serve as tribo-positive and tribo-negative layers in the triboelectrification process, respectively. The PDMS film was patterned with a series of spacers, which separate and support the two electrification layers to realize the contact−separation motions of the top/bottom parts and thereby the generation of electrical outputs. All of the hydrogel/elastomer interfaces were treated with BP for tough bonding. The detailed preparation process and photographs of the TENG are shown in Figure S5 and Figure S6, respectively. It is obvious that the highly flexible TENG is able to be attached conformly to various curvy surfaces of the human body (Figure 5b), which provides possibility to be integrated with wearable and flexible electronics.[35,60−62]

As shown schematically in Figure 5c, the middle PDMS and Ecoflex layers will be electrified upon their contact due to the applied external pressure, generating static surface negative and positive charges, respectively.[53] Once the pressure is removed, the upper/lower parts will bounce back and the two electrified surfaces will be separated, due to the existence of elastic spacers. Meantime, ions in the two hydrogel electrodes will move to screen the static charges, and induced electrons will

DOI: 10.1021/acsnano.8b00108
ACS Nano XXXX, XXX, XXX−XXX

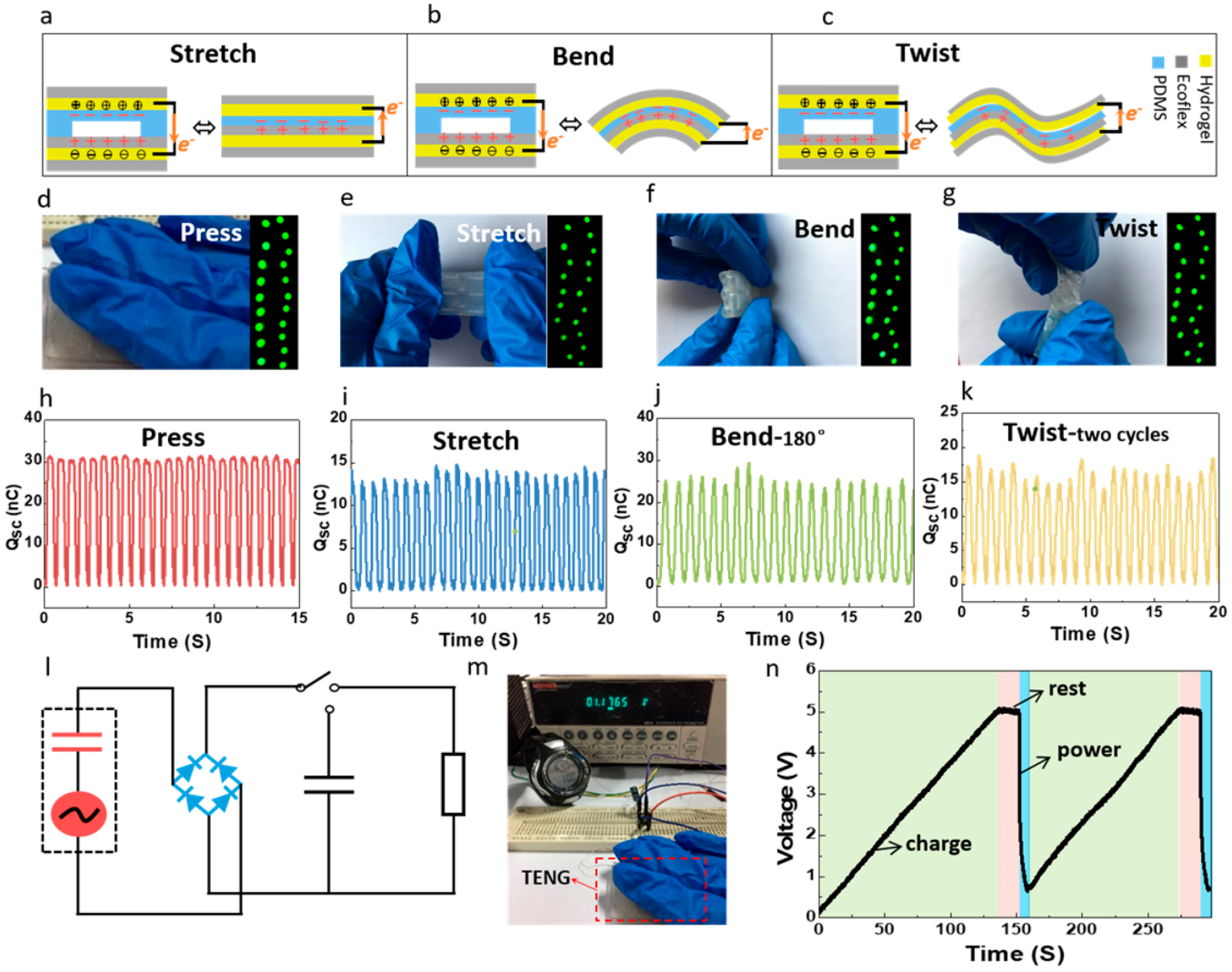

Figure 6. Harvesting multiple types of motion/deformation energies by the two-electrode TENG. Schematic diagrams showing the working mechanism of the contact−separation TENG when it is under (a) stretching, (b) bending, and (c) twisting motions. Photographs and Q_{SC} when the TENG is working under (d and h) pressing, (e and i) stretching, (f and j) bending, and (g and k) twisting motions. (l) The equivalent circuit and (m) image of a self-charging system that uses the energy harvested from TENG to power electronics. (n) Voltage profile of a 2.2-μF capacitor being charged by the TENG and powering the electronic watch.

flow through the external circuit. Repeated deformation of the TENG will then lead to the generation of continuous alternative currents. When the moving dielectric film is in contact with another dielectric film, both V_{oc} and Q_{sc} are 0. When the top electrode is moving far away, V_{oc} and Q_{sc} can be derived as[57]

$$V_{oc} = -\sigma A/C_o \quad (3)$$

$$Q_{sc} = -\sigma A \quad (4)$$

The contact−separation mode TENG generated the peak V_{oc} of 100 V (Figure 5d), peak Q_{sc} of 32 nC (Figure 5e), and peak I_{sc} of 0.36 μA (Figure 5f). As the external loading resistance increases, the current density amplitude decreases; while the output power density of the device reaches the peak value of 44 mW/m^2 at an optimum load resistance of 600 MΩ (Figure S7a). It is clearly seen that the output voltage of the TENG does not exhibit obvious change after ∼5000 cycles (for 60 min) of repeated contact−separation motion (Figure S7b). After storage at an RH of ∼26% at 30 °C for 3 days and 21 days, the electrical output performances of the hydrogel−elastomer hybrid based TENG show no noticeable degradation, as shown in Figure S7c. This stable long-term performance and antidehydration performance are attributed to the excellent elastic properties of the whole systems and toughly bonded hydrogel/elastomer interfaces.

The soft TENG can be used for harvesting mechanical energy, especially the energy of human motions. Thanks to the flexibility and stretchability, the hydrogel−elastomer based TENG can operate under multiple deformations without any mechanical damage (Figure 6a−k). Twenty green light-emitting diodes (LEDs) connected in series can be easily lit by pressing (Figure 6d, Supporting Movie S1), stretching (Figure 6e, Supporting Movie S2), bending (Figure 6f, Supporting Movie S3), or twisting (Figure 6g, Supporting Movie S4) the TENG. The corresponding Q_{sc} based on the motions are presented in Figure 6h,i,j,k, respectively. When the TENG works under the pressing motion, it has a higher electrical output than the other three situations. According to the schematic illustration of the working mechanisms under diverse motions (Figure 5c and

DOI: 10.1021/acsnano.8b00108
ACS Nano XXXX, XXX, XXX−XXX

Figure 6a,b,c), the high electrical outputs mainly depend on the much larger relative displacement between the two electrodes, along with the much more effective contact area.[63]

Furthermore, the electrical output of the hydrogel−elastomer-based TENG can be stored in energy storage devices (such as capacitors) to power up portable electronics. The hydrogel−elastomer based TENG is pressed with a frequency of 1 to 2 Hz to charge a 2.2-μF capacitor and then power an electronic watch through the equivalent circuit in Figure 6l. Initially, the voltage of the capacitor increases linearly to 5 V in 150 s, and then it is capable of powering an electronic watch for about 15 s while the voltage of the capacitor drops rapidly (Figure 6m). As the TENG is continuously pressed, the capacitor can be charged back to 5 V, suggesting that the harvested energy can not only drive the watch but also sufficiently charge the capacitor. This demonstration indicates that the device can act as a fully self-powered and sustainable electronic system, with great potential in deformable, portable and wearable electronics.

CONCLUSIONS

In summary, soft, flexible and stretchable TENGs with toughly bonded hydrogel−elastomer hybrids were developed for potential applications as energy-harvesting skin. The robust bonding interface between the hydrogel electrode and the elastomer electrification layer, achieved by the surface modification by BP, ensured the stable electrical output of the hybrid-based TENG. Meantime, the dehydration rate of the sandwiched hydrogel can decrease by 73.2%−78.6% as compared to that of the uncoated one. The single-electrode TENG energy skin has a high transparency (90%) and an ultrathin thickness (380 μm), enabling it to conformally attach to human skin and deform with the body's movement. The contact−separation mode TENG is capable of harvesting energy from an arbitrary mechanical movement (press, stretch, bend, and twist) to drive the self-powered electronics. But, because of the use of Ecoflex film, the two-electrode TENG in this work is not transparent. A new transparent tribo-positive elastomer will be needed in the future. The applicability of the designed TENG as a sustainable energy source for self-powered electronics has been demonstrated by powering commercial electronic devices. Therefore, the practically viable energy harvesting skin exhibited in this work is highly promising for powering next-generation soft electronics.

METHODS

Fabrication of Pregel Solution (Ionic Conductor). The PAAm−alginate hydrogel was prepared according to the method reported previously: 12.05 wt % AAm, 1.95 wt % sodium alginate, 0.017 wt % MBAA, and 0.2 wt % Irgacure 2959 were mixed to prepare the PAAm−alginate pregel solution. The mixture was stirred fully, and air bubbles were removed through vacuum pumping.

Bonding Hydrogels on Elastomers. The surfaces of elastomers were treated by BP in ethanol solution according to the method reported previously. First, the elastomer surfaces were cleaned with methanol and deionized water thoroughly, followed by soaking the elastomer fully in BP solution (10 wt % in ethanol) for 2 min at room temperature. Thereafter, the elastomer was washed with methanol for three times and dried completely with nitrogen gas. The acrylic mold was placed on the treated elastomer film. The pregel solution was poured into the acrylic mold, and then an ionic cross-linkers solution (mixing 0.172 g of calcium sulfate with 8 mL of deionized water) was injected into the pregel solution. Then another treated elastomer was added to the incomplete cured hydrogel followed by UV irradiation of the hydrogel in the UV chamber (350 nm ultraviolet) for 40 min, during which time the PAAm network was covalently cross-linked and bonded onto the elastomer surface.

Fabrication of the Single-Electrode TENG. The PDMS film (20 μm thick) was prepared by spin-coating the mixture of Sylgard 184 base and curing agents (10:1 by weight) followed with 80 °C treatment for 2 h. Then the TENG was assembled by sandwiching the PAAm−alginate hydrogel with the two PDMS films. Cu wire was attached to the hydrogel for electrical connection.

Fabrication of the Contact-Separation TENG. The PDMS spacer (2 mm thick) was prepared by pouring the mixture of Sylgard 184 base and curing agents (10:1 by weight) into the arclic mold followed by an 80 °C treatment for 2 h. The Ecoflex film (90 μm thick) was prepared by spin-coating the mixture of Ecoflex oo-2o A and Ecoflex oo-2o B (1:1 by weight) followed with 60 °C treatment for 2 h. The top electrode was fabricated by sandwiching the PAAm−alginate hydrogel with the elastomer film and the PDMS spacer. The bottom electrode was fabricated by sandwiching the PAAm−alginate hydrogel with elastomer films. The final device was fabricated by sandwiching the upper part and the bottom part. Cu wire was attached to the hydrogel for an electrical connection.

Characterization and Measurements. A step motor (LinMot E1100) was used to provide the input of mechanical motions. For all the tests of energy generation of the TENG, the pressure (100 kPa), speed (0.2 m/s), and frequency (~1.5 Hz) of the step motor were fixed. The voltage and charge quantity were recorded by a Keithley electrometer 6514, and the current was recorded with a Stanford low-noise preamplifier SR570. The mechanical tensile test and stretch cycling test of the hydrogel−elastomer hybrid were conducted by an ESM301/Mark-10 system. For the antidehydration test, the dry environment was created by storing dehydrated desiccants in an oven at 30 °C, RH 26%. The RH was monitored with a hygrometer, and the weights of the samples were recorded every 12 h. The electrochemical impedance spectroscopy of the hydrogel was measured using a potentiostat (Metrohm PGSTAT302N), by sandwiching the hydrogel layer (area = 2.5 cm × 2.5 cm, thickness = 2 mm) between two indium tin oxide (ITO) glass pieces.

ASSOCIATED CONTENT

Supporting Information

The Supporting Information is available free of charge on the ACS Publications website at DOI: 10.1021/acsnano.8b00108.

Chemical reaction process when treating elastomer with BP, tensile test of hydrogel/elastomer hybrid, EIS measurement of the hydrogel, resistance changes of the hydrogel electrode with the tensile strain, partial electrical output performance of TENGs, preparation process and optical images of the contact−separation (PDF)

The contact−separation TENG harvesting energy from arbitrary human motions (press) (AVI)

The contact−separation TENG harvesting energy from arbitrary human motions (stretch) (AVI)

The contact−separation TENG harvesting energy from arbitrary human motions (bend) (AVI)

The contact−separation TENG harvesting energy from arbitrary human motions (twist) (AVI)

AUTHOR INFORMATION

Corresponding Authors

*E-mail: puxiong@binn.cas.cn.

*E-mail: huweiguo@binn.cas.cn.

*E-mail: zlwang@gatech.edu.

ORCID

Xiong Pu: 0000-0002-1254-8503

DOI: 10.1021/acsnano.8b00108
ACS Nano XXXX, XXX, XXX−XXX

Weiguo Hu: 0000-0002-8614-0359
Zhong Lin Wang: 0000-0002-5530-0380

Notes

The authors declare no competing financial interest.

ACKNOWLEDGMENTS

The authors thank the National Key Research and Development Program of China (No. 2016YFA0202703), National Natural Science Foundation of China (Grant Nos. 51432005, 61574018, and 51603013), Beijing Municipal Science & Technology Commission (Z171100000317001), the "Thousands Talents" program for pioneer researcher and his innovation team, China, and the Youth Innovation Promotion Association of CAS, "Hundred Talents Program" of CAS for support.

REFERENCES

(1) Kim, D. H.; Lu, N.; Ma, R.; Kim, Y. S.; Kim, R. H.; Wang, S.; Wu, J.; Won, S. M.; Tao, H.; Islam, A.; et al. Epidermal Electronics. *Science* **2011**, *333*, 838−843.
(2) Tee, B. C.; Wang, C.; Allen, R.; Bao, Z. An Electrically and Mechanically Self-Healing Composite with Pressure-and Flexion-Sensitive Properties for Electronic Skin Applications. *Nat. Nanotechnol.* **2012**, *7*, 825−832.
(3) Huang, X.; Liu, Y.; Cheng, H.; Shin, W. J.; Fan, J. A.; Liu, Z.; Lu, C. J.; Kong, G. W.; Chen, K.; Patnaik, D.; et al. Materials and Designs for Wireless Epidermal Sensors of Hydration and Strain. *Adv. Funct. Mater.* **2014**, *24*, 3846−3854.
(4) Chortos, A.; Liu, J.; Bao, Z. Pursuing Prosthetic Electronic Skin. *Nat. Mater.* **2016**, *15*, 937−950.
(5) Wehner, M.; Truby, R. L.; Fitzgerald, D. J.; Mosadegh, B.; Whitesides, G. M.; Lewis, J. A.; Wood, R. J. An Integrated Design and Fabrication Strategy for Entirely Soft, Autonomous Robots. *Nature* **2016**, *536*, 451−455.
(6) Liang, J.; Li, L.; Niu, X.; Yu, Z.; Pei, Q. Elastomeric Polymer Light-Emitting Devices and Displays. Nat. *Nat. Photonics* **2013**, *7*, 817−824.
(7) White, M. S.; Kaltenbrunner, M.; Głowacki, E. D.; Gutnichenko, K.; Kettlgruber, G.; Graz, I.; Aazou, S.; Ulbricht, C.; Egbe, D. A. M.; Miron, M. C.; Major, Z.; Scharber, M. C.; Sekitani, T.; Someya, T.; Bauer, S.; Sariciftci, N. S. Ultrathin, Highly Flexible and Stretchable PLEDs. *Nat. Photonics* **2013**, *7*, 811−816.
(8) Yokota, T.; Zalar, P.; Kaltenbrunner, M.; Jinno, H.; Matsuhisa, N.; Kitanosako, H.; Tachibana, Y.; Yukita, W.; Koizumi, M.; Someya, T. Ultraflexible Organic Photonic Skin. *Sci. Adv.* **2016**, *2*, e1501856.
(9) Liu, M.; Pu, X.; Jiang, C.; Liu, T.; Huang, X.; Chen, L.; Du, C.; Sun, J.; Hu, W.; Wang, Z. L. Large-Area All-Textile Pressure Sensors for Monitoring Human Motion and Physiological Signals. *Adv. Mater.* **2017**, *29*, 1703700.
(10) Pu, X.; Liu, M.; Li, L.; Han, S.; Li, X.; Jiang, C.; Du, C.; Luo, J.; Hu, W.; Wang, Z. L. Wearable Textile-Based in-Plane Micro-supercapacitors. *Adv. Energy Mater.* **2016**, *6*, 1601254.
(11) Fang, H.; Yu, K. J.; Gloschat, C.; Yang, Z.; Song, E.; Chiang, C. H.; Zhao, J.; Won, S. M.; Xu, S.; Trumpis, M.; Zhong, Y.; Han, S.; Xue, Y.; Xu, D.; Choi, S.; Cauwenberghs, G.; Kay, M.; Huang, Y.; Viventi, J.; Efimov, I.; et al. Capacitively Coupled Arrays of Multiplexed Flexible Silicon Transistors for Long-Term Cardiac Electrophysiology. *Nat. Biomed. Eng.* **2017**, *1*, 0038.
(12) Zheng, Q.; Shi, B.; Fan, F.; Wang, X.; Yan, L.; Yuan, W.; Wang, S.; Liu, H.; Li, Z.; Wang, Z. L. *In Vivo* Powering of Pacemaker by Breathing-Driven Implanted Triboelectric Nanogenerator. *Adv. Mater.* **2014**, *26*, 5851−5856.
(13) Lou, Z.; Chen, S.; Wang, L.; Shi, R.; Li, L.; Jiang, K.; Chen, D.; Shen, G. Ultrasensitive and Ultraflexible E-Skins with Dual Functionalities for Wearable Electronics. *Nano Energy* **2017**, *38*, 28−35.
(14) Pu, X.; Hu, W.; Wang, Z. L. Toward Wearable Self-Charging Power Systems: The Integration of Energy-Harvesting and Storage Devices. *Small* **2018**, *14*, 1702817.
(15) Sun, N.; Wen, Z.; Zhao, F.; Yang, Y.; Shao, H.; Zhou, C.; Shen, Q.; Feng, K.; Peng, M.; Li, Y.; Sun, X. H. All Flexible Electrospun Papers Based Self-Charging Power System. *Nano Energy* **2017**, *38*, 210−217.
(16) Song, Y.; Cheng, X.; Chen, H.; Huang, J.; Chen, X.; Han, M.; Su, Z.; Meng, B.; Song, Z.; Zhang, H. Integrated Self-Charging Power Unit with Flexible Supercapacitor and Triboelectric Nanogenerator. *J. Mater. Chem. A* **2016**, *4*, 14298−14306.
(17) Wang, Z. L.; Chen, J.; Lin, L. Progress in Triboelectric Nanogenerators as a New Energy Technology and Self-Powered Sensors. *Energy Environ. Sci.* **2015**, *8*, 2250−2282.
(18) Hinchet, R.; Seung, W.; Kim, S. W. Recent Progress on Flexible Triboelectric Nanogenerators for Self-Powered Electronics. *ChemSusChem* **2015**, *8*, 2327−2344.
(19) Fan, F. R.; Tang, W.; Wang, Z. L. Flexible Nanogenerators for Energy Harvesting and Self-Powered Electronics. *Adv. Mater.* **2016**, *28*, 4283−4305.
(20) Pu, X.; Li, L.; Song, H.; Du, C.; Zhao, Z.; Jiang, C.; Cao, G.; Hu, W.; Wang, Z. L. A Self-Charging Power Unit by Integration of a Textile Triboelectric Nanogenerator and a Flexible Lithium-Ion Battery for Wearable Electronics. *Adv. Mater.* **2015**, *27*, 2472−2478.
(21) Chen, J.; Zhu, G.; Yang, W.; Jing, Q.; Bai, P.; Yang, Y.; Hou, T. C.; Wang, Z. L. Harmonic-Resonator-Based Triboelectric Nanogenerator as a Sustainable Power Source and a Self-Powered Active Vibration Sensor. *Adv. Mater.* **2013**, *25*, 6094−6099.
(22) Zhu, G.; Chen, J.; Zhang, T.; Jing, Q.; Wang, Z. L. Radial-Arrayed Rotary Electrification for High Performance Triboelectric Generator. *Nat. Commun.* **2014**, *5*, 3426.
(23) Liang, Q.; Zhang, Q.; Yan, X.; Liao, X.; Han, L.; Yi, F.; Ma, M.; Zhang, Y. Recyclable and Green Triboelectric Nanogenerator. *Adv. Mater.* **2017**, *29*, 1604961.
(24) Shen, Q.; Xie, X.; Peng, M.; Sun, N.; Shao, H.; Zheng, H.; Wen, Z.; Sun, X. Self-Powered Vehicle Emission Testing System Based on Coupling of Triboelectric and Chemoresistive Effects. *Adv. Funct. Mater.* **2018**, 1703420.
(25) Yang, P. K.; Lin, L.; Yi, F.; Li, X.; Pradel, K. C.; Zi, Y.; Wu, C. I.; He, J. H.; Zhang, Y.; Wang, Z. L. A flexible, Stretchable and Shape-Adaptive Approach for Versatile Energy Conversion and Self-Powered Biomedical Monitoring. *Adv. Mater.* **2015**, *27*, 3817−3824.
(26) He, X.; Zi, Y.; Guo, H.; Zheng, H.; Xi, Y.; Wu, C.; Wang, J.; Zhang, W.; Lu, C.; Wang, Z. L. A Highly Stretchable Fiber-Based Triboelectric Nanogenerator for Self-Powered Wearable Electronics. *Adv. Funct. Mater.* **2017**, *27*, 1604378.
(27) Kwak, S. S.; Kim, H.; Seung, W.; Kim, J.; Hinchet, R.; Kim, S. W. Fully Stretchable Textile Triboelectric Nanogenerator with Knitted Fabric Structures. *ACS Nano* **2017**, *11*, 10733−10741.
(28) Parida, K.; Kumar, V.; Jiangxin, W.; Bhavanasi, V.; Bendi, R.; Lee, P. S. Highly Transparent, Stretchable, and Self-Healing Ionic-Skin Triboelectric Nanogenerators for Energy Harvesting and Touch Applications. *Adv. Mater.* **2017**, *29*, 1702181.
(29) Kim, C. C.; Lee, H. H.; Oh, K. H.; Sun, J. Y. Highly Stretchable, Transparent Ionic Touch Panel. *Science* **2016**, *353*, 682−687.
(30) Sun, J. Y.; Keplinger, C.; Whitesides, G. M.; Suo, Z. Ionic Skin. *Adv. Mater.* **2014**, *26*, 7608−7614.
(31) Lee, K. Y.; Gupta, M. K.; Kim, S. W. Transparent Flexible Stretchable Piezoelectric and Triboelectric Nanogenerators for Powering Portable Electronics. *Nano Energy* **2015**, *14*, 139−160.
(32) Lai, Y. C.; Deng, J.; Niu, S.; Peng, W.; Wu, C.; Liu, R.; Wen, Z.; Wang, Z. L. Electric Eel-Skin-Inspired Mechanically Durable and Super-Stretchable Nanogenerator for Deformable Power Source and Fully Autonomous Conformable Electronic-Skin Applications. *Adv. Mater.* **2016**, *28*, 10024−10032.
(33) Yi, F.; Lin, L.; Niu, S.; Yang, P. K.; Wang, Z.; Chen, J.; Zhou, Y.; Zi, Y.; Wang, J.; Liao, Q.; Zhang, Y.; Wang, Z. L. Stretchable-Rubber-Based Triboelectric Nanogenerator and Its Application as Self-

DOI: 10.1021/acsnano.8b00108
ACS Nano XXXX, XXX, XXX−XXX

Powered Body Motion Sensors. *Adv. Funct. Mater.* **2015**, *25*, 3688−3696.
(34) Hwang, B. U.; Lee, J. H.; Trung, T. Q.; Roh, E.; Kim, D. I.; Kim, S. W.; Lee, N. E. Transparent Stretchable Self-Powered Patchable Sensor Platform with Ultrasensitive Recognition of Human Activities. *ACS Nano* **2015**, *9*, 8801−8810.
(35) Yi, F.; Wang, X.; Niu, S.; Li, S.; Yin, Y.; Dai, K.; Zhang, G.; Lin, L.; Wen, Z.; Guo, H.; et al. A Highly Shape-Adaptive, Stretchable Design Based on Conductive Liquid for Energy Harvesting and Self-Powered Biomechanical Monitoring. *Sci. Adv.* **2016**, *2*, e1501624.
(36) Dong, K.; Wang, Y. C.; Deng, J.; Dai, Y.; Zhang, S. L.; Zou, H.; Gu, B.; Sun, B.; Wang, Z. L. A Highly Stretchable and Washable All-Yarn-Based Self-Charging Knitting Power Textile Composed of Fiber Triboelectric Nanogenerators and Supercapacitors. *ACS Nano* **2017**, *11*, 9490−9499.
(37) Pu, X.; Liu, M.; Chen, X.; Sun, J.; Du, C.; Zhang, Y.; Zhai, J.; Hu, W.; Wang, Z. L. Ultrastretchable, Transparent Triboelectric Nanogenerator as Electronic Skin for Biomechanical Energy Harvesting and Tactile Sensing. *Sci. Adv.* **2017**, *3*, e1700015.
(38) Caló, E.; Khutoryanskiy, V. V. Biomedical Applications of Hydrogels: A Review of Patents and Commercial Products. *Eur. Polym. J.* **2015**, *65*, 252−267.
(39) Deligkaris, K.; Tadele, T. S.; Olthuis, W.; van den Berg, A. Hydrogel-Based Devices for Biomedical Applications. Sens. *Sens. Actuators, B* **2010**, *147*, 765−774.
(40) Kawai, A.; Hirakawa, M.; Abe, T.; Obi, K.; Shibuya, K. Specific Solvent Effects on the Structure and Reaction Dynamics of Benzophenone Ketyl Radical. *J. Phys. Chem. A* **2001**, *105*, 9628−9636.
(41) Schneider, M. H.; Tran, Y.; Tabeling, P. Benzophenone Absorption and Diffusion in Poly (Dimethylsiloxane) and Its Role in Graft Photo-Polymerization for Surface Modification. *Langmuir* **2011**, *27*, 1232−1240.
(42) Yuk, H.; Zhang, T.; Parada, G. A.; Liu, X.; Zhao, X. Skin-Inspired Hydrogel-Elastomer Hybrids with Robust Interfaces and Functional Microstructures. *Nat. Commun.* **2016**, *7*, 12028.
(43) Shi, M.; Zhang, J.; Chen, H.; Han, M.; Shankaregowda, S. A.; Su, Z.; Meng, B.; Cheng, X.; Zhang, H. Self-Powered Analogue Smart Skin. *ACS Nano* **2016**, *10*, 4083−4091.
(44) Bai, Y.; Chen, B.; Xiang, F.; Zhou, J.; Wang, H.; Suo, Z. Transparent Hydrogel with Enhanced Water Retention Capacity by Introducing Highly Hydratable Salt. *Appl. Phys. Lett.* **2014**, *105*, 151903.
(45) Chen, X.; Song, Y.; Chen, H.; Zhang, J.; Zhang, H. An Ultrathin Stretchable Triboelectric Nanogenerator with Coplanar Electrode for Energy Harvesting and Gesture Sensing. *J. Mater. Chem. A* **2017**, *5*, 12361−12368.
(46) Fan, F. R.; Lin, L.; Zhu, G.; Wu, W.; Zhang, R.; Wang, Z. L. Transparent Triboelectric Nanogenerators and Self-Powered Pressure Sensors Based on Micropatterned Plastic Films. *Nano Lett.* **2012**, *12*, 3109−3114.
(47) Kim, S.; Gupta, M. K.; Lee, K. Y.; Sohn, A.; Kim, T. Y.; Shin, K. S.; Kim, D.; Kim, S. K.; Lee, K. H.; Shin, H. J.; Kim, D. W.; Kim, S. W. Transparent Flexible Graphene Triboelectric Nanogenerators. *Adv. Mater.* **2014**, *26*, 3918−3925.
(48) Liang, Q.; Yan, X.; Gu, Y.; Zhang, K.; Liang, M.; Lu, S.; Zheng, X.; Zhang, Y. Highly Transparent Triboelectric Nanogenerator for Harvesting Water-Related Energy Reinforced by Antireflection Coating. *Sci. Rep.* **2015**, *5*, 9080.
(49) Zhao, Z.; Pu, X.; Du, C.; Li, L.; Jiang, C.; Hu, W.; Wang, Z. L. Freestanding Flag-Type Triboelectric Nanogenerator for Harvesting High-Altitude Wind Energy from Arbitrary Directions. *ACS Nano* **2016**, *10*, 1780−1787.
(50) Zheng, Q.; Shi, B.; Fan, F.; Wang, X.; Yan, L.; Yuan, W.; Wang, S.; Liu, H.; Li, Z.; Wang, Z. L. *In Vivo* Powering of Pacemaker by Breathing-Driven Implanted Triboelectric Nanogenerator. *Adv. Mater.* **2014**, *26*, 5851−5856.
(51) Tang, Y.; Zheng, Q.; Chen, B.; Ma, Z.; Gong, S. A New Class of Flexible Nanogenerators Consisting of Porous Aerogel Films Driven by Mechanoradicals. *Nano Energy* **2017**, *38*, 401−411.
(52) Seol, M. L.; Woo, J. H.; Jeon, S. B.; Kim, D.; Park, S. J.; Hur, J.; Choi, Y. K. Vertically Stacked Thin Triboelectric Nanogenerator for Wind Energy Harvesting. *Nano Energy* **2015**, *14*, 201−208.
(53) Wen, Z.; Shen, Q.; Sun, X. Nanogenerators for Self-Powered Gas Sensing. *Nano-Micro Lett.* **2017**, *9*, 45.
(54) Ye, B. U.; Kim, B. J.; Ryu, J.; Lee, J. Y.; Baik, J. M.; Hong, K. Electrospun Ion Gel Nanofibers for Flexible Triboelectric Nanogenerator: Electrochemical Effect on Output Power. *Nanoscale* **2015**, *7*, 16189−16194.
(55) Wang, S.; Lin, L.; Wang, Z. L. Triboelectric Nanogenerators as Self-Powered Active Sensors. *Nano Energy* **2015**, *11*, 436−462.
(56) Chun, J.; Kim, J. W.; Jung, W. S.; Kang, C. Y.; Kim, S. W.; Wang, Z. L.; Baik, J. M. Mesoporous Pores Impregnated with Au Nanoparticles as Effective Dielectrics for Enhancing Triboelectric Nanogenerator Performance in Harsh Environments. *Energy Environ. Sci.* **2015**, *8*, 3006−3012.
(57) Y Yang, B.; Zeng, W.; Peng, Z. H.; Liu, S. R.; Chen, K.; Tao, X. M. A Fully Verified Theoretical Analysis of Contact-Mode Triboelectric Nanogenerators as a Wearable Power Source. *Adv. Energy Mater.* **2016**, *6*, 1600505.
(58) Niu, S.; Wang, Z. L. Theoretical Systems of Triboelectric Nanogenerators. *Nano Energy* **2015**, *14*, 161−192.
(59) Niu, S.; Liu, Y.; Wang, S.; Lin, L.; Zhou, Y. S.; Hu, Y.; Wang, Z. L. Theory of Sliding-Mode Triboelectric Nanogenerators. *Adv. Mater.* **2013**, *25*, 6184−6193.
(60) Pu, X.; Song, W.; Liu, M.; Sun, C.; Du, C.; Jiang, C.; Huang, X.; Zou, D.; Hu, W.; Wang, Z. L. Wearable Power-Textiles by Integrating Fabric Triboelectric Nanogenerators and Fiber-Shaped Dye-Sensitized Solar Cells. *Adv. Energy Mater.* **2016**, *6*, 1601048.
(61) Pu, X.; Li, L.; Liu, M.; Jiang, C.; Du, C.; Zhao, Z.; Hu, W.; Wang, Z. L. Wearable Self-Charging Power Textile Based on Flexible Yarn Supercapacitors and Fabric Nanogenerators. *Adv. Mater.* **2016**, *28*, 98−105.
(62) Wen, Z.; Yeh, M. H.; Guo, H.; Wang, J.; Zi, Y.; Xu, W.; Deng, J.; Zhu, L.; Wang, X.; Hu, C.; et al. Self-Powered Textile for Wearable Electronics by Hybridizing Fiber-Shaped Nanogenerators, Solar Cells, and Supercapacitors. *Sci. Adv.* **2016**, *2*, e1600097.
(63) Yi, F.; Wang, J.; Wang, X.; Niu, S.; Li, S.; Liao, Q.; Xu, Y.; You, Z.; Zhang, Y.; Wang, Z. L. Stretchable and Waterproof Self-Charging Power System for Harvesting Energy from Diverse Deformation and Powering Wearable Electronics. *ACS Nano* **2016**, *10*, 6519−6525.

DOI: 10.1021/acsnano.8b00108
ACS Nano XXXX, XXX, XXX−XXX